Preparation and mechanical performance of graphene platelet reinforced titanium nanocomposites for high temperature applications

Liu, Jian; Wu, Mingxia; Yang, Yi; Yang, Gang; Yan, Haixue; Jiang, Kyle

DOI:
10.1016/j.jallcom.2018.06.148

Document Version
Peer reviewed version

Citation for published version (Harvard):
Liu, J, Wu, M, Yang, Y, Yang, G, Yan, H & Jiang, K 2018, 'Preparation and mechanical performance of graphene platelet reinforced titanium nanocomposites for high temperature applications' Journal of Alloys and Compounds, vol. 765, pp. 1111-1118. https://doi.org/10.1016/j.jallcom.2018.06.148

Accepted Manuscript

Preparation and mechanical performance of graphene platelet reinforced titanium nanocomposites for high temperature applications

Jian Liu, Mingxia Wu, Yi Yang, Gang Yang, Haixue Yan, Kyle Jiang

PII: S0925-8388(18)32269-2

DOI: 10.1016/j.jallcom.2018.06.148

Reference: JALCOM 46484

To appear in: *Journal of Alloys and Compounds*

Received Date: 30 March 2018

Revised Date: 10 June 2018

Accepted Date: 14 June 2018

Please cite this article as: J. Liu, M. Wu, Y. Yang, G. Yang, H. Yan, K. Jiang, Preparation and mechanical performance of graphene platelet reinforced titanium nanocomposites for high temperature applications, *Journal of Alloys and Compounds* (2018), doi: 10.1016/j.jallcom.2018.06.148.

Preparation and mechanical performance of graphene platelet reinforced titanium nanocomposites for high temperature applications

Jian Liu[1]*, Mingxia Wu[1], Yi Yang[1], Gang Yang[1]*, Haixue Yan[2], Kyle Jiang[3]

[1]School of Manufacturing Science and Engineering, Sichuan University, China, 610065

[2]School of Materials Science and Engineering, University of London, Queen Mary. London E1 4NS

[3]Department of Mechanical Engineering, School of Engineering, University of Birmingham, UK, B15 2TT

Abstract: In this paper graphene platelet (GPL)-reinforced titanium（Ti）composites (GPL/Ti) were prepared using spark plasma sintering to evaluate a new type of structural material. The microstructure, mechanical properties and high temperature compressive properties of the GPL/Ti composites were studied. It was found that GPLs are well dispersed in the Ti matrix and the introduction of GPL results in the refinement of the Ti microstructure. Although x-ray diffraction results imply no traceable reaction products are produced in GPL/Ti composites, scanning electron and element analyses

* Corresponding author: E-mail addresses: liujian@scu.edu.cn (Jian Liu); yanggang@scu.edu.cn (gang yang)

indicate titanium carbide particles are found along the interface between the GPL and Ti matrix. Compressive tests show that GPL/Ti composites exhibit higher yield strength and better compressive performance than the pure Ti samples. A maximum increase of approximately 43% and 37% in yield strength and compressive strength are achieved, respectively. Raman analysis suggests the reaction between GPLs and Ti results in the reduction in the number of the layers in graphene structure. The presented work suggests that GPL/Ti might be of great potential to be used as a structural material in various engineering fields.

Key words: Graphene platelet; Titanium; Composites; Spark plasma sintering;

Compressive property

1. Introduction

Titanium and its alloys have been widely used materials and have applications covering aerospace parts, hip implants, automotive and marine components due to its low density, high strength and excellent corrosion resistance[1-10]. In addition, it has been considered a very suitable material for elevated applications. However, high temperature applications usually entail improved mechanical performance of titanium materials. Titanium matrix composites are therefore produced with the aim to impart the additional property to the titanium matrix [11]. The concept of metal matrix composites (MMCs) reinforced with various nano fillers was proposed many years ago and have shed light on the development of novel structural materials for a variety of applications[12-16]. Generally, mechanical performance of the MMCs to a large extent is dependent on the reinforcements selected and reinforcements with high young's

modulus are usually desired[17]. A number of reinforcing particles or filler have been incorporated into the Ti matrix to produce composite materials. Wang et al. used the spark plasma sintering (SPS) technique to successfully fabricate carbon nanotube (CNT) reinforced Ti composites and found that the addition of 0.4 wt% CNTs could result in an increase of 61.5% in compressive strength [18]. The significant improvement in the mechanical properties was attributed to the grain refinement and reinforcing effects of CNTs. Li et.al prepared the Ti composites reinforced with titanium carbides (TiC) particles and titanium boride (TiB_2) whiskers and reported that the Ti composite with compressive strength of 1138MPa was obtained with an introduction of 13.6 vol% hybrid fillers of TiC and TiB_2 [1]. It was suggested that the tensile strength was considerably enhanced due to the refined microstructure, homogenous distribution of the reinforcements and the cohesive strength between the matrix and the reinforcement. Luo et al. used a novel method combining resol nanosphere coating and conventional powder metallurgy to produce TiC nanoplatelet-reinforced Ti composites and found that the Ti composites with ultimate strength of 2.54 GPa and yield strength of 1.52 GPa were achieved [19]. The ultrahigh strength of the TiC/Ti composites primarily arose from the locally aligned TiC nanoplatelets.

Graphene since discovered in 2004 has received enormous attention globally and its excellent electrical and mechanical properties make it a suitable candidate to be used in a variety of applications [20-22]. Compared to monolayer graphene, GPLs are stacked graphene with thickness of up to approximately 100 nm. It is reported that the young's modulus of GPLs with thickness of 2-8 nm is approximately 0.5Tpa [23], which is higher than many metallic materials. Compared with the many other filling materials (CNT, TiC and TiB_2), GPLs have higher strength and larger specific surface area and

can cause a good match between strength and ductility in the as-fabricated composites [9]. It is expected that analogous to conventional ceramic composites reinforced with micrometric fibres, the incorporation of GPLs can lead to considerable improvement in the compressive property of the metallic materials. Attempts have been made to produce GPL-reinforced metallic composites[4, 8-10, 24]. Mu produced Ti composites with a low content (0.1wt%) of GPLs utilizing SPS and a hot rolling process and reported an approximately 54% improvement in the tensile strength. The significant enhancement in the mechanical property was attributed to the load transfer of GPLs, texture strengthening and grain refinement[24]. Jingyue fabricated GPL/aluminum(Al) composites using powder metallurgy and a hot extrusion process and found that an addition of 0.3wt% GPLs could produce a 62% enhancement in tensile strength of the Al and the ultimate tensile strength could be as high as 249MPa [25]. Muhammad Rashad et al. prepared the GPL/magnesium composites through pressurelessing sintering in a purified argon atmosphere and reported that compared to the pure magnesium samples, the GPL/magnesium composite containing 0.3wt% produced showed increase of 131%, 49.5 and 74.2% in Young's modulus, yield strength and failure strain respectively[26]. Dandan et al. fabricated GPL/copper composites using SPS and found that the composite with introduction of 0.5 wt% GPLs exhibited an increase of 49.1% in yield strength [27]. Shin et al. produced the GPL/Al composite samples using the hot rolling process and found that the strength of the composites increases with the specific surface area on the composites and the composites containing 0.7 vol% GPLs exhibit 440 MPa of tensile strength [28]. Shufeng Li et al. fabricated graphite powder/Ti composite using the SPS and hot extrusion techniques and reported that increase of around 30% and 2% in yield strength and tensile strength were achieved

respectively [2]. Cao et al. produced the GPL/Ti composites utilizing hot static pressing and isothermal forging processes and found that remarkable improvements in the tensile and yield strength were obtained with the minor addition of GPLs.

As a rapid powder consolidation process with unique characteristics in comparison with conventional sintering methods, SPS process enables metal matrix composites with good properties to be fabricated by providing much higher rapid heating and cooling rates, a shorter holding time and a higher pressure at a relatively lower sintering temperature. These advantages would efficiently help prohibit the grain growth during the sintering process and prevent the formation of byproducts due to the reaction between the carbon filler and Ti matrix. To the best knowledge of the authors, there are scarce reports on Ti composites reinforced by GPLs and the compressive performance of the GPL/Ti composites has not explored yet.

In this study, the Ti composites reinforced with GPLs were prepared using SPS and the high temperature compressive performance of the GPL/Ti composite was investigated using Gleeble 1500D (Dynamic Systems Inc, USA) thermal simulation machine. Microstructures of the composites were examined by optical and scanning electron microscopy (SEM). Phase composition of the composites was determined by x-ray diffraction (XRD) and energy-dispersive detector (EDS). Structural integrity of the GPLs was assessed by Raman spectroscopy.

2. Experimental procedure

2.1 Starting materials

Pure Ti powder （99.5%, 45 μm, sigma Aldrich, UK) was used as starting materials. GPLs powder procured from Graphene Industries Ltd, Manchester, UK, with an average

thickness 6-8 nm and 15–25 μm in diameter were used as the reinforcing materials in the present study. Ball milling process was performed to produce powder mixtures with 0.25wt%GPLs at 100 rpm in a planetary ball mill (PM 100, Retsch, UK) for 3 hours. The milling was carried out in a cylindrical alumina container using zirconia balls under a ball-to-powder weight ratio of 2. The image of the powder mixtures is shown in Fig. 1. As shown in Figure 1a, much powder with size smaller than the original raw powder (45 μm) is noted, implying that powder was fractured during the ball milling process. It is suggested that both cold working and cold welding are present in the ball milling process of metal powder [29]. The cold working tends to fracture the powder particle while the cold welding has the tendency to increase the particle size. Specifically, the cold-welding becomes predominant and leads to the agglomeration of the particles with the increasing ball-milling time. Nevertheless, similar to CNT, it is expected that GPLs can play a role as a grinding aid during the ball milling process by forming a network of weak interfaces between GPLs and the Ti matrix due to the small size and flexibility of GPLs [13]. This weak interface network formed because of the GPLs can act as a crack initiator to prevent the agglomeration of the Ti powder and weaken van der Waals forces between GPLs, resulting in the improved dispersion of GPLs and Ti powder.

2.2 Sintering and compressive experiments

The powder mixtures and pure Ti powder were consolidated by SPS (HPD 25/1 furnace, FCT Systeme, Germany) process at 850 ºC at a heating rate 50 ºC for half an hour under vacuum (<5 Pa) and a uniaxial pressure of 50MPa was applied throughout the sintering

cycle. The sintered specimen possess a diameter of 60 mm and a height of 10 mm. Afterwards, the specimen were cut into cylinders with a diameter of 6 mm and a height of 9 mm. Compression experiments were then carried out on a gleeble-1500D (Dynamic Systems Inc, USA) thermal simulation machine to evaluate the mechanical performance of the sintered samples. A heating rate of 30 ºC/s was used to heat the samples to the preset temperatures between 25 to 800 ºC and compressed at a strain rate of $10^{-3}s^{-1}$. The processing parameters were selected based on the previous reports with the aim to achieve a high degree of densification [2, 30-32] and at least three samples were tested to obtain the mechanical properties of the sintered materials.

2.3 Materials characterizations

The sintered samples were ground and polished to 0.5µm using silicon carbide papers and diamond suspension. The bulk density of the samples was measured using the Archimedes method with ethanol as the immersion medium. Vickers hardness tests were carried out under a 1kg force. Microstructures of the composites were examined by optical microscopy and SEM. Phase composition of the composites was determined by XRD. A Raman Microscope (RenishawInVia Reflex and Witec Alpha 300R) was used to characterize the GPLs in the powder mixtures and sintered samples with the 532 nm laser wavelength excitation.

3 Results and discussion

3.1 Compressive properties of the prepared samples

Typical stress–strain curves of compressed pure Ti and Ti/GPLs composites at various

temperatures are given in Figure 2. It is evidently observed that the compressive strength of pure Ti and Ti/GPLs composites decrease significantly with the increase of temperature. This fact can be explained by diffusion-controlled creep phenomenon, which suggests elevated temperatures would significantly reduce hardening effects and render the plastic deformation to proceed easily [33, 34]. Under the action of compressive stress and high temperatures Ti atoms at grain boundaries which are parallel to the compressive stress axis can be diffused into another side of grain boundaries which are perpendicular to the compressive stress axis, causing a plastic compression of Ti grains along the compressive axis and increase of the cross sectional area of the test specimen quickly [11].

On the other hand, although the true stress increases linearly with the true strain during the initial compressing test for all of samples, which indicates the identical slope of the linear portion of the curve and Young's modulus for both the pure Ti and GPL/Ti composites, it should be noted that the yield stress and the compressive strength of GPL-reinforced Ti composites at the same temperature are considerably higher than those of pure Ti. A summarization of average yield and compressive strength of the pure Ti and GPL/Ti composite is given in Table 1. It can be noticed that a maximum compressive strength of 1345 MPa and a maximum yield strength of 1122 MPa are

Table 1 Mechanical properties of the GPL/Ti composite and pure Ti at various temperatures

Compressing temperature (°C)	Yield strength (MPa) (Ti)	Yield strength (MPa) (GPL/Ti)	Compressive strength (MPa) (Ti)	Compressive strength (MPa) (GPL/Ti)
25	927±22	1122±28	1172±24	1345±33
200	331±11	390±21	688±27	704±29
400	236±10	338±11	347±15	476±19
600	144±9	180±14	159±11	191±15
800	34±2	41±3	37±3	47±5

obtained for the GPL/Ti composite compressed at room temperature respectively. In particular, when sample are compressed at 400 °C, it is found that an increase of approximately 43% and an increase of around 37% in yield strength and compressive strength are achieved. The significant improvement in the strength of the Ti matrix material is closely related to the addition of the reinforcing agent of GPLs and main strength mechanisms are expected to be associated with the microstructure, solid solution of carbon and dispersion strengthening of GPLs.

Meanwhile, a further observation of the curves reveal that the variation of the true stress with the true strain exhibit the same trend for samples compressed at 25, 200 and 400°C, which shows that the true stress initially increases linearly and then parabolically with the true strain while the compressive stress decreases or remain stable around a certain value after the linear increase stage for samples compressed at 600 and 800°C respectively. The different tendencies of these curves are intimately associated with the dynamic process involving work hardening and recovery. The initial stage indicates the elastic deformation and follows the Hooke's law while parabolic stage implies that the

work hardening effect is more appreciable than the recovery effect in the plastic deformation process. In addition, usually built-up of dislocation networks would occur in the parabolic stage and requires a higher compressive stress for the deformation to carry on. Nonetheless, the decreasing and stable trends in the later stage of the compressing at higher temperatures suggest the recovery process plays a more important role than the hardening effect, leading to the annihilation of dislocations and softening of the materials. As a result, only a relatively low compressive stress is needed for the later plastic deformation process.

3.2 Microstructures of the prepared samples

Figure 3 shows the optical microstructure images of the compressed pure Ti and GPL/Ti composites at different compression temperatures. It can be noticed that with the increasing temperature a coarse microstructure tends to be obtained for both pure Ti and GPL/Ti composites and at the same compression temperature GPL/Ti composites exhibit a finer microstructure than the Ti matrix. The coarse microstructure of the pure Ti is related to the recovery process and coarsening of Ti grain occurred during compression process. Recovery is often strongly dependent
on the time and temperature. Since the compression time is very short, the temperature will be the major influencing factor and compression temperatures higher than 400°C result in a much more coarse microstructure for the pure Ti than the lower temperatures. On the other hand, the microstructures of GPL/Ti composites compressed at varied temperatures exhibit a far smaller difference in comparison with those of pure Ti. The

very small change in microstructure is mainly attributed to the pinning effect of GPLs. As shown in Figure 4, GPLs tend to distribute at the boundaries of the Ti grains (a-d) or embed in the Ti matrix (f-g), which prevents the rapid growth of the matrix grains at high temperatures and strengthens the Ti matrix. Meanwhile, particles (Fig.4e) formed in the interface between GPLs and Ti matrix are noticed. It is expected that due to the close affinity between Ti and carbon atoms, when a carbon source is introduced in the Ti matrix, titanium carbide (TiC) particles often will be produced because of the reaction between Ti and GPLs and can provide additional inhibition of the grain growth. Typical XRD patterns of the compressed pure Ti and Ti/GPLs composites are shown in Figure 5. It can be seen that only Ti peaks are found in all of samples and no traceable TiC is detected at high processing temperatures, implying that the amount of the formation of the TiC compound during both the sintering and compression processes is very small. Peak shift is noticed and attributed to the dissolution of carbon into hexagonal closed packing (HCP) lattice of α-Ti. The lattice parameters of a-axis and c-axis of α -Ti HCP structure estimated based upon the least squares methods is complied in Table 2. It implies that carbon atom originating from GPLs and/or in situ formed TiC dispersoids can be dissolved into Ti matrix, resulting in expansion of Ti lattice parameters.

Table 2 Lattice parameters of pure Ti and GPL/Ti composites processed at various temperatures

Compressing temperature (°C)	a-Axis (Ti)	c-Axis (Ti)	c/a (Ti)	a-Axis (GPL/Ti)	c-Axis (GPL/Ti)	c/a (GPL/Ti)
25	2.95466	4.69185	1.5879	2.9555	4.68905	1.5866
200	2.9594	4.70685	1.5905	2.95738	4.70166	1.5898
400	2.95839	4.71427	1.5879	2.95601	4.70255	1.5908
600	2.95907	4.70583	1.5903	2.9522	4.70024	1.5921
800	2.9598	4.70957	1.5912	2.95495	4.6958	1.5891

The Raman spectra of the pristine GPL and GPLs in the compressed samples are compared in Figure 6. It can be seen that the raw GPLs exhibit a typical D, G and 2D bands and the intensity of the 2D band is significantly lower than that of G band, indicating a multilayer graphene structure. The GPLs in compressed samples present much higher spectrum backgrounds compared to the pristine GPL. The increased spectrum backgrounds can be attributed to interaction of GPLs with the Ti matrix during the sintering process, which tends to form the TiC particles. This can be further corroborated by the D peak split, indicating a change in defect density in graphene.

3.3 Microstructures of the prepared samples

The densities of the pure Ti and GPL/Ti composites after compression are given in Table 3. It can be observed that all of samples reach a high density and most of the pure

Ti and GPL/Ti composites processed at high temperatures possess a higher density than the pure Ti at the room temperature, indicating a higher temperature tends to further the consolidation of the materials. Nonetheless, GPL/Ti composites compressed at higher temperatures exhibit a relatively slight decrease in the density in comparison with those processed at the room temperature. The minor change in the density might be associated with the reactions between GPLs and the Ti matrix.

Table 3 Densities and porosity of the pure Ti and GPL/Ti composites

Materials	Density (g/cm^3)/(porosity)				
	(25ºC)	(200ºC)	(400ºC)	(600ºC)	(800ºC)
Pure Ti	4.46 (1.11%)	4.51(0%)	4.47(0.89%)	4.48(0.67%)	4.47(0.89%)
GPL/Ti	4.50(0%)	4.46(0.89%)	4.49(0.22%)	4.47(0.67%)	4.46(0.89%)

Table 4. Hardness of the pure Ti, GPL/Ti and area neighboring GPLs

Materials	Vickers hardness				
	(25ºC)	(200ºC)	(400ºC)	(600ºC)	(800ºC)
Area around GPLs	450±16	420±20	460±25	438±22	425±17
GPL/Ti matrix	435±28	402±15	413±22	378±19	375±13
Pure Ti	370±22	350±18	356±17	335±23	343±13

To evaluate the reinforcing effects induced by GPLs and the interaction between the GPL and matrix, hardness in the Ti matrix and area neighboring the GPLs in the GPL/Ti composites were provided in Figure 6. It can be observed that the addition of GPLs leads to significant increase in hardness of the Ti matrix and the maximum

increase in hardness is obtained when the GPL/Ti composite is compressed at a temperature of 400ºC. In addition, hardness of both the pure Ti and GPL/Ti composites compressed at high temperatures is lower than that processed at the room temperature respectively. What should be noted is that both pure Ti and GPL/Ti composites compressed at 400ºC exhibit higher hardness than those processed at 200ºC, which can be interpreted by the fact that the recovery and nucleation take place at this temperature and significantly strengthen the matrix of the materials. With the processing temperatures increasing to higher than 400ºC, grain coarsening might occur and lead to the degradation of the mechanical properties, which explains the relatively lower hardness at 400ºC than at 200ºC. Hardness in the area neighboring GPLs reveals that a high processing temperature tends to promote the reaction between the GPLs and Ti matrix and facilitates the formation of TiC particles which can act as additional reinforcing agents. This account for the fact hardness around GPLs processed at temperatures of 400, 600 and 800ºC is higher than that at 200ºC.

4. Discussion

When it comes to composites materials, either metal matrices or ceramic matrices, microstructures and interfaces between the reinforcing agents and matrices will have significant effects on the mechanical properties of the materials. In terms of the microstructure, the strengthening mechanism due to refined microstructure usually is estimated based upon the Hall–Petch relationship[35, 36]:

$$\sigma = \sigma_0 + kD^{-1/2} \quad (1)$$

σ_0 is a constant stress and k is a materials constant. D is a mean grain diameter of the Ti matrix.

It is evident that a refined microstructure with a small grain size of matrix tends to possess a high strength. Previous studies indicate that the k constant at the room temperature is nearly comparable to that at 200ºC, which implies that the strain hardening effect plays a dominant role in the yield stress at relatively low processing temperature during the compression process while after the compression temperature increasing to higher than 200ºC, the k constant is inclined to decrease and the recovery process would exist a significant influence on the plastic deformation process at high temperatures [2, 11]. Another important strengthening factor is the GPLs introduced in the composites. Reportedly GPLs possess an extraordinarily high Young's modulus, the uniform distribution of GPLs in the matrix boundaries will certainly enhance the strength of the Ti matrix considerably in addition to the refining effect on the microstructure. Meanwhile, additional strengthening effects can be produced by forming solid solution of carbon and TiC because of the high affinity of carbon atoms with Ti matrix. Carbon is an effective strengthener below its limit of solubility in α-Ti. Above this limit, carbon presents as TiC particles. The maximum equilibrium solubility of carbon in α-Ti from is reported to be 0.4 wt.% and the dissolved carbon atoms usually can causes the lattice distortion of Ti atoms[11].

Carbon solid solution strengthening effects usually can be estimated according to Friedel–Fleischer model and almost are same for all the composites with a low carbon

content. Nonetheless, an introduction of a relatively high content of carbon source is likely to promote the formation of the TiC dispersoids. The standard free energy (ΔG) for the formation of TiC particles by reaction between Ti and carbon at various temperatures can be expressed as the following equation and given in Table 5 [2].

$$\Delta G = -184571.8 + 41.382T - 5.042T\ln T + 2.425 \times 10^{-3}T^2 - 9.79 \times \frac{10^5}{T} \quad (T<1666^oC) \quad (2)$$

Table 5. Gibbs free energy for the reaction between GPLs and Ti

T(ºC)	25	200	400	600	800	900
ΔG(KJ/mol)	-184.48	-181.21	-179.17	-177.53	-176.04	-175.33

It can be seen that the all of the Gibbs free energy for the reaction between GPLs and Ti at various temperatures are below zero and indicates that in situ formation of TiC is spontaneous at room and elevated temperatures, explaining the observation of particles in the grain boundaries between GPLs and Ti (Figure 4e). The formation of TiC particles are expected to retard Ti grain coarsening and enhance the stability of strength of the composites by the pinning and dispersion strengthening mechanisms during elevated temperature compression. Meanwhile, TiC dispersoids can prevent the recrystallization of new grains during the long time annealing owing to the fact the pinning pressure induced by TiC is higher than driving pressure for recrystallization nucleation of new grain [11]. On the other hand, since TiC particles are a hard intermetallic phase with a high Young's modulus and can not be plastically deformed, an additional strengthening effect to the Ti matrix is therefore likely to be provided to increase the compressive strength as well as the hardness. However, the formed TiC particles may act as the sites of crack initiation and result in a low percentage elongation

for the composites during a tensile test due to the poor plasticity. In particular, when a carbon source is introduced, the reaction between the carbon source and the Ti matrix is normally incomplete, leading to the presence of unreacted carbon in the core of TiC particles. It is expected that pores are likely to be formed between the layered structure of GPLs caused by weak bonding (van der Waals force) under residual stress, due to different coefficients of thermal expansion between Ti matrix and TiC, which significantly deteriorates the mechanical properties of the composites [2]. Potential approaches to retard the formation of TiC particles include a use of a low processing temperature or coating a layer of materials less reactive to Ti on the carbon source[37]. A lower temperature can reduce the tendency of Ti to react with the carbon source and a layer of less reactive coating can prevent the direct contact of Ti with the carbon source, leading to the formation of less TiC particles. Nevertheless, TiC can strengthen the Ti matrix by refining the matrix microstructure and hindering the dislocation slip [2] and may find applications in aerospace and biomedical industries [38, 39]. For the matrices of both pure Ti and GPL/Ti composites and the area neighboring the GPLs in the composites, the hardness initially decrease and then increase, followed by a downward trend with the increasing compression temperature. The initial decrease and the downward trend in hardness can be attributed to the recovery process which alleviates the stress within the materials and reduce the dislocation density within the Ti matrix. Such softening mechanisms surely would result in a decrease in hardness of both the pure Ti and GPL/Ti composites. The increase in hardness at a compression temperature

of 400°C is expected to be associated with the renucleation, refined microstructure and the amount of TiC formed during the compression process. The nucleation of new grains tends to decrease the grain size of the matrix and increase the hardness of both the pure Ti and GPL/Ti composites. The Ti matrix microstructure refined due to the addition of GPLs and the formation of the hard TiC phase owing to the interaction between the GPLs and Ti matrix are other reasons contributing to the improvement of the hardness for the GPL/Ti composites. In particular, the strengthening effect becomes evident in the area close to the interface between GPLs and Ti in the GPL/Ti composites where a high hardness is noted.

What should be noted is that the formation of TiC is at expense of the carbon atoms in GPLs and would damage the structural integrity of the GPLs. Usually the ratio of intensities of 2D to G peaks (I_{2D}/I_G) and D to G (I_D/I_G) peaks in Raman spectra can be used to evaluate the graphene structure. I_{2D}/I_G often tends to decrease with the increasing number of graphene layers while I_D/I_G reveal the defect density in GPLs [19]. Raman parameters are compiled in Table 6. It can be observed that I_{2D}/I_G of GPLs in the composites processed at high temperatures is higher than that compressed at the room temperature, indicating a high temperature promotes the reaction between the GPLs and Ti and reduce the layers of the GPLs. Nonetheless, a lower I_D/I_G is noted for GPLs processed at high temperature, which implies that interaction between GPLs and Ti reduce the defect density in GPLs. On the other hand, it is noted that G and 2D bands of GPLs processed at high temperatures shift to higher wave number as compared to those

of GPLs compressed at room temperature. The shift of G peak to higher wave number can be mainly attributed to the thermal stress acting on GPLs incurred during thermal contraction of Ti matrix.

Table 6. Raman parameters of the GPLs in the GPL/Ti composites

Temperature	ν_G	ν_{2D}	I_D/ I_G	I_{2D}/ I_G
25	1572	2713	0.72	1.12
200	1582	2713	0.74	1.78
400	1572	2715	0.51	1.12
600	1578	2725	0.61	1.13
800	1580	2722	0.65	1.20

It was suggested that when a low addition of GPLs was added in the Ti matrix, the improvement in mechanical properties contributed by the grain refinement is much smaller compared to the load transfer strengthening of the GPLs [24]. Meanwhile, due to a very small loading of GPLs added, the amount of TiC formed during the processing is expected to be very small and its reinforcing effect to the Ti matrix is insignificant. Therefore, the load transfer strengthening is considered as the main reinforcing mechanism for the GPL/Ti composites in this study. The reinforcing effect induced by the GPLs can be roughly assessed based upon the following question and the reinforcing efficiency at various temperatures is summarized in Table 7.

$$R_a = \frac{\sigma_c - \sigma_m^*}{V_f \times \sigma_m^*} \quad (3)$$

where R_a is the reinforcing efficiency, σ_c is the strength of the composite, σ_m^* the strength of the pure metal, V_f the volume fraction of the reinforcing phase.

It can be seen that the reinforcing efficiency for both yield strength and tensile strength nearly exhibit the same trends. It decreases when the temperature increases to 200ºC and

increases with the temperature further increasing to 400ºC, which is followed by decreases with the continuous increase in temperature.

Table 7 Reinforcing efficiency induced by the GPLs at various temperatures

Compression temperature (ºC)	Ra (Yield strength)	Ra (Tensile strength)
25	30.26	28.70
200	29.46	25.58
400	35.81	34.29
600	31.25	30.03
800	30.15	31.75

4. **Conclusions**

In this study GPL/Ti composites were fabricated using spark plasma sintering and the mechanical performance and the microstructure were investigated. The results indicate that GPLs are homogeneously distributed in Ti matrix. TiC particles are found in the interface between the GPLs and Ti matrix due to the reaction between them at various processing temperatures. GPL/Ti composites present higher yield strength and better compressive performance than the pure Ti samples. Raman analysis suggests close interaction between GPLs and Ti matrix leads to the reduction in the layers of graphene structure. The presented study indicates that the lightweight GPL/Ti composites might find various applications that demand excellent high temperature performance.

Acknowledgements

This publication is based on the research funded by the National Natural Science Foundation of China (Grant No. 51675357and Grant No. 51605317).

References

[1] S.F. Li, K. Kondoh, H. Imai, B. Chen, L. Jia, J. Umeda, Microstructure and mechanical properties of P/M titanium matrix composites reinforced by in-situ synthesized TiC-TiB, Mat Sci Eng a-Struct 628 (2015) 75-83.

[2] S.F. Li, B. Sun, H. Imai, T. Mimoto, K. Kondoh, Powder metallurgy titanium metal matrix composites reinforced with carbon nanotubes and graphite, Compos Part a-Appl S 48 (2013) 57-66.

[3] B. Wang, L.J. Huang, L. Geng, X.D. Rong, Compressive behaviors and mechanisms of TiB whiskers reinforced high temperature Ti60 alloy matrix composites, Mat Sci Eng a-Struct 648 (2015) 443-451.

[4] Z. Cao, X. Wang, J. Li, Y. Wu, H. Zhang, J. Guo, S. Wang, Reinforcement with graphene nanoflakes in titanium matrix composites, J Alloy Compd 696 (2017) 498-502.

[5] X.G. Fan, H.J. Zheng, Y. Zhang, Z.Q. Zhang, P.F. Gao, M. Zhan, J. Liu, Acceleration of globularization during interrupted compression of a two-phase titanium alloy, Mat Sci Eng a-Struct 720 (2018) 214-224.

[6] P.L. Narayana, S.-W. Kim, J.-K. Hong, N.S. Reddy, J.-T. Yeom, Tensile properties of a newly developed high-temperature titanium alloy at room temperature and 650 °C, Mat Sci Eng a-Struct 718 (2018) 287-291.

[7] Y. Sun, G. Luo, J. Zhang, C. Wu, J. Li, Q. Shen, L. Zhang, Phase transition, microstructure and mechanical properties of TC4 titanium alloy prepared by plasma activated sintering, J Alloy Compd 741 (2018) 918-926.

[8] X.N. Mu, H.N. Cai, H.M. Zhang, Q.B. Fan, F.C. Wang, Z.H. Zhang, Y. Wu, Y.X. Ge, S. Chang, R. Shi, Y. Zhou, D.D. Wang, Uniform dispersion of multi-layer graphene reinforced pure titanium matrix composites via flake powder metallurgy, Mat Sci Eng a-Struct 725 (2018) 541-548.

[9] M. Gürbüz, T. Mutuk, Effect of process parameters on hardness and microstructure of graphene reinforced titanium composites, J Compos Mater 52(4) (2017) 543-551.

[10] Z. Hu, F. Chen, J. Xu, Z. Ma, H. Guo, C. Chen, Q. Nian, X. Wang, M. Zhang, Fabricating graphene-titanium composites by laser sintering PVA bonding graphene titanium coating: Microstructure and mechanical properties, Compos Part B: Eng 134 (2018) 133-140.

[11] K. Kondoh, T. Threrujirapapong, J. Umeda, B. Fugetsu, High-temperature properties of extruded titanium composites fabricated from carbon nanotubes coated titanium powder by spark plasma sintering and hot extrusion, Compos Sci Technol 72(11) (2012) 1291-1297.

[12] S.T. Mileiko, High temperature oxide-fibre/metal-matrix composites, Mater Chem Phys 210 (2018) 353-361.

[13] C.A. Isaza Merino, J.E. Ledezma Sillas, J.M. Meza, J.M. Herrera Ramirez, Metal matrix composites reinforced with carbon nanotubes by an alternative technique, J Alloy Compd 707 (2017) 257-263.

[14] J. Liu, Y. Yang, K. Feng, D. Lu, Study on the effect of current on reactive sintering of the W–C–Co mixture under an electric field, J Alloy Compd 476(1) (2009) 207-212.

[15] B. Chen, J. Shen, X. Ye, L. Jia, S. Li, J. Umeda, M. Takahashi, K. Kondoh, Length effect of carbon nanotubes on the strengthening mechanisms in metal matrix composites, Acta Mater 140 (2017) 317-325.

[16] V.A. Popov, E.V. Shelekhov, A.S. Prosviryakov, M.Y. Presniakov, B.R. Senatulin, A.D. Kotov, M.G. Khomutov, Particulate metal matrix composites development on the basis of in situ synthesis of TiC reinforcing nanoparticles during mechanical alloying, J Alloy Compd 707 (2017) 365-370.

[17] K. Jiang, J. Li, J. Liu, Electrochemical codeposition of graphene platelets and nickel for improved corrosion resistant properties, RSC Adv 4(68) (2014) 36245-36252.

[18] F.C. Wang, Z.H. Zhang, Y.J. Sun, Y. Liu, Z.Y. Hu, H. Wang, A.V. Korznikov, E. Korznikova, Z.F. Liu, S. Osamu, Rapid and low temperature spark plasma sintering synthesis of novel carbon nanotube reinforced titanium matrix composites, Carbon 95 (2015) 396-407.

[19] S.D. Luo, Q. Li, J. Tian, C. Wang, M. Yan, G.B. Schaffer, M. Qian, Self-assembled, aligned TiC nanoplatelet-reinforced titanium composites with outstanding compressive properties, Scripta Mater 69(1) (2013) 29-32.

[20] J. Liu, H.X. Yan, K. Jiang, Mechanical properties of graphene platelet-reinforced alumina ceramic composites, Ceram Int 39(6) (2013) 6215-6221.

[21] J. Liu, H.X. Yan, M.J. Reece, K. Jiang, Toughening of zirconia/alumina composites by the addition of graphene platelets, J Eur Ceram Soc 32(16) (2012) 4185-4193.

[22] J. Liu, Y. Yang, H. Hassanin, N. Jumbu, S.A. Deng, Q. Zuo, K.L. Jiang,

Graphene-Alumina Nanocomposites with Improved Mechanical Properties for Biomedical Applications, Acs Appl Mater Inter 8(4) (2016) 2607-2616.

[23] I.W. Frank, D.M. Tanenbaum, A.M. Van der Zande, P.L. McEuen, Mechanical properties of suspended graphene sheets, J Vac Sci Technol B 25(6) (2007) 2558-2561.

[24] X.N. Mu, H.M. Zhang, H.N. Cai, Q.B. Fan, Z.H. Zhang, Y. Wu, Z.J. Fu, D.H. Yu, Microstructure evolution and superior tensile properties of low content graphene nanoplatelets reinforced pure Ti matrix composites, Mat Sci Eng a-Struct 687 (2017) 164-174.

[25] J.Y. Wang, Z.Q. Li, G.L. Fan, H.H. Pan, Z.X. Chen, D. Zhang, Reinforcement with graphene nanosheets in aluminum matrix composites, Scripta Mater 66(8) (2012) 594-597.

[26] M. Rashad, F.S. Pan, H.H. Hu, M. Asif, S. Hussain, J. She, Enhanced tensile properties of magnesium composites reinforced with graphene nanoplatelets, Mat Sci Eng a-Struct 630 (2015) 36-44.

[27] D.D. Zhang, Z.J. Zhan, Preparation of graphene nanoplatelets-copper composites by a modified semi-powder method and their mechanical properties, J Alloy Compd 658 (2016) 663-671.

[28] S.E. Shin, H.J. Choi, J.H. Shin, D.H. Bae, Strengthening behavior of few-layered graphene/aluminum composites, Carbon 82 (2015) 143-151.

[29] K. Chu, C.-c. Jia, L.-k. Jiang, W.-s. Li, Improvement of interface and mechanical properties in carbon nanotube reinforced Cu–Cr matrix composites, Mater Design 45

(2013) 407-411.

[30] O. Ertorer, T.D. Topping, Y. Li, W. Moss, E.J. Lavernia, Nanostructured Ti Consolidated via Spark Plasma Sintering, Metall Mater Trans A 42(4) (2011) 964-973.

[31] M. Shahedi Asl, A. Sabahi Namini, A. Motallebzadeh, M. Azadbeh, Effects of sintering temperature on microstructure and mechanical properties of spark plasma sintered titanium, Mater Chem Phys 203 (2018) 266-273.

[32] F. Xue, S. Jiehe, F. Yan, C. Wei, Preparation and elevated temperature compressive properties of multi-walled carbon nanotube reinforced Ti composites, Mat Sci Eng a-Struct 527(6) (2010) 1586-1589.

[33] M.J.R. Barboza, E.A.C. Perez, M.M. Medeiros, D.A.P. Reis, M.C.A. Nono, F.P. Neto, C.R.M. Silva, Creep behavior of Ti–6Al–4V and a comparison with titanium matrix composites, Mat Sci Eng a-Struct 428(1) (2006) 319-326.

[34] Y. Estrin, G. Gottstein, L.S. Shvindlerman, Diffusion controlled creep in nanocrystalline materials under grain growth, Scripta Mater 50(7) (2004) 993-997.

[35] W. Xu, L.P. Dávila, Tensile nanomechanics and the Hall-Petch effect in nanocrystalline aluminium, Mat Sci Eng a-Struct 710 (2018) 413-418.

[36] H. Zhou, H. Cui, Q.-H. Qin, H. Wang, Y. Shen, A comparative study of mechanical and microstructural characteristics of aluminium and titanium undergoing ultrasonic assisted compression testing, Mat Sci Eng a-Struct 682 (2017) 376-388.

[37] J. Fang, W. Zha, M. Kang, S. Lu, L. Cui, S. Li, Microwave absorption response of nickel/graphene nanocomposites prepared by electrodeposition, J Mater Sci 48(23)

(2013) 8060-8067.

[38] M. Xia, A. Liu, Z. Hou, N. Li, Z. Chen, H. Ding, Microstructure growth behavior and its evolution mechanism during laser additive manufacture of in-situ reinforced (TiB+TiC)/Ti composite, J Alloy Compd 728 (2017) 436-444.

[39] F. Ma, C. Wang, P. Liu, W. Li, X. Liu, X. Chen, K. Zhang, Q. Han, Microstructure and mechanical properties of Ti matrix composite reinforced with 5 vol.% TiC after various thermo-mechanical treatments, J Alloy Compd 758 (2018) 78-84.

Figures and Tables Captions

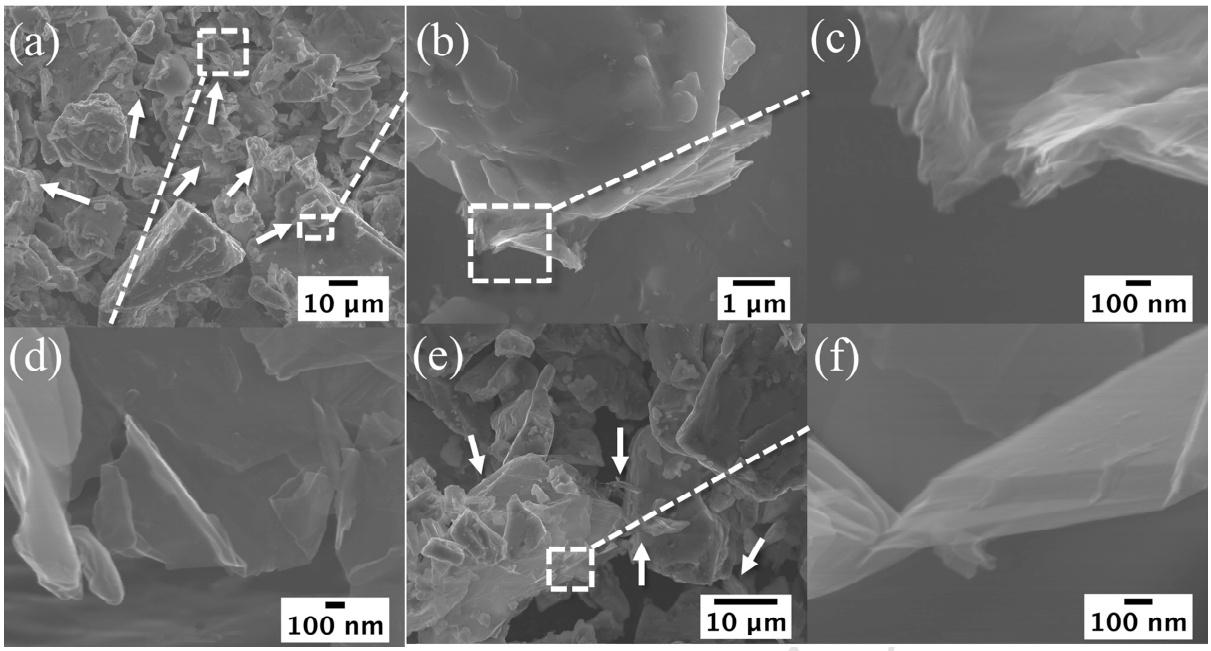

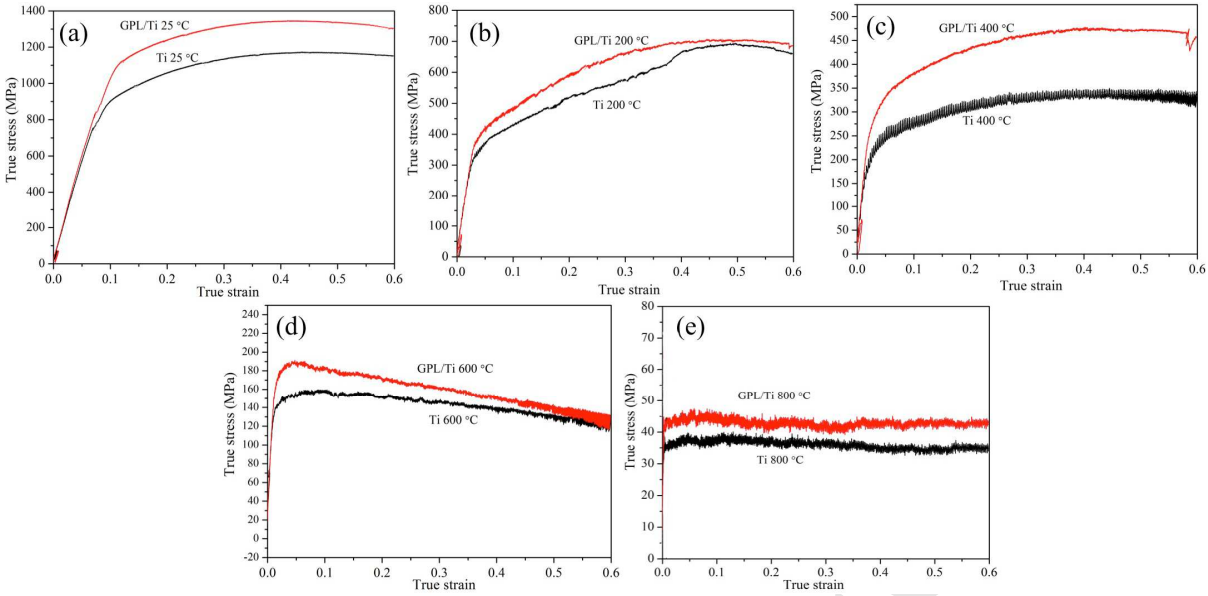

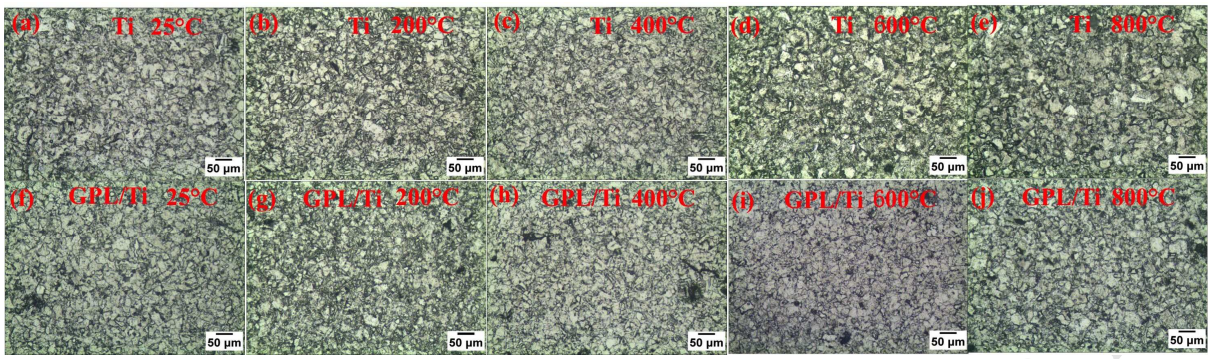

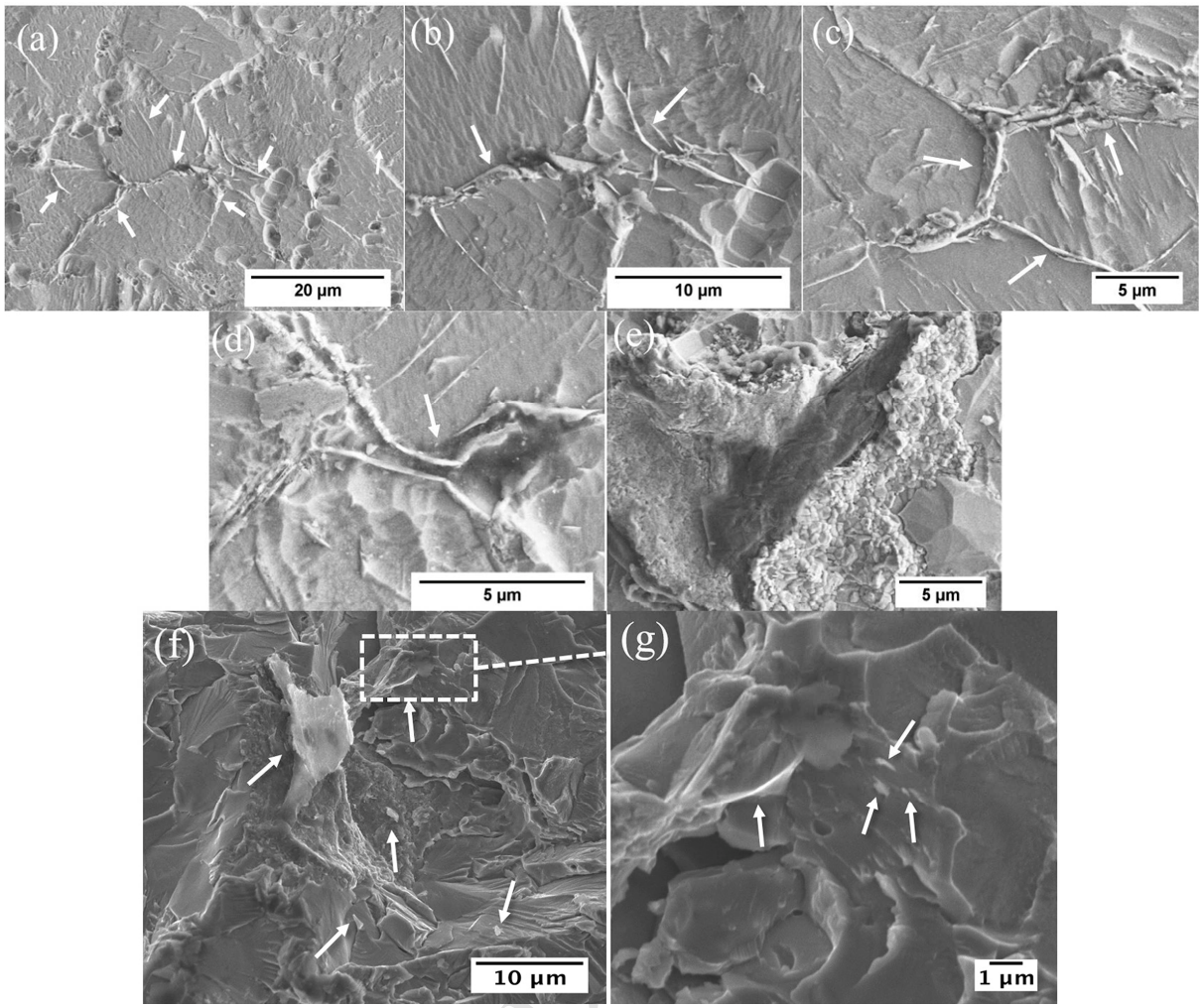

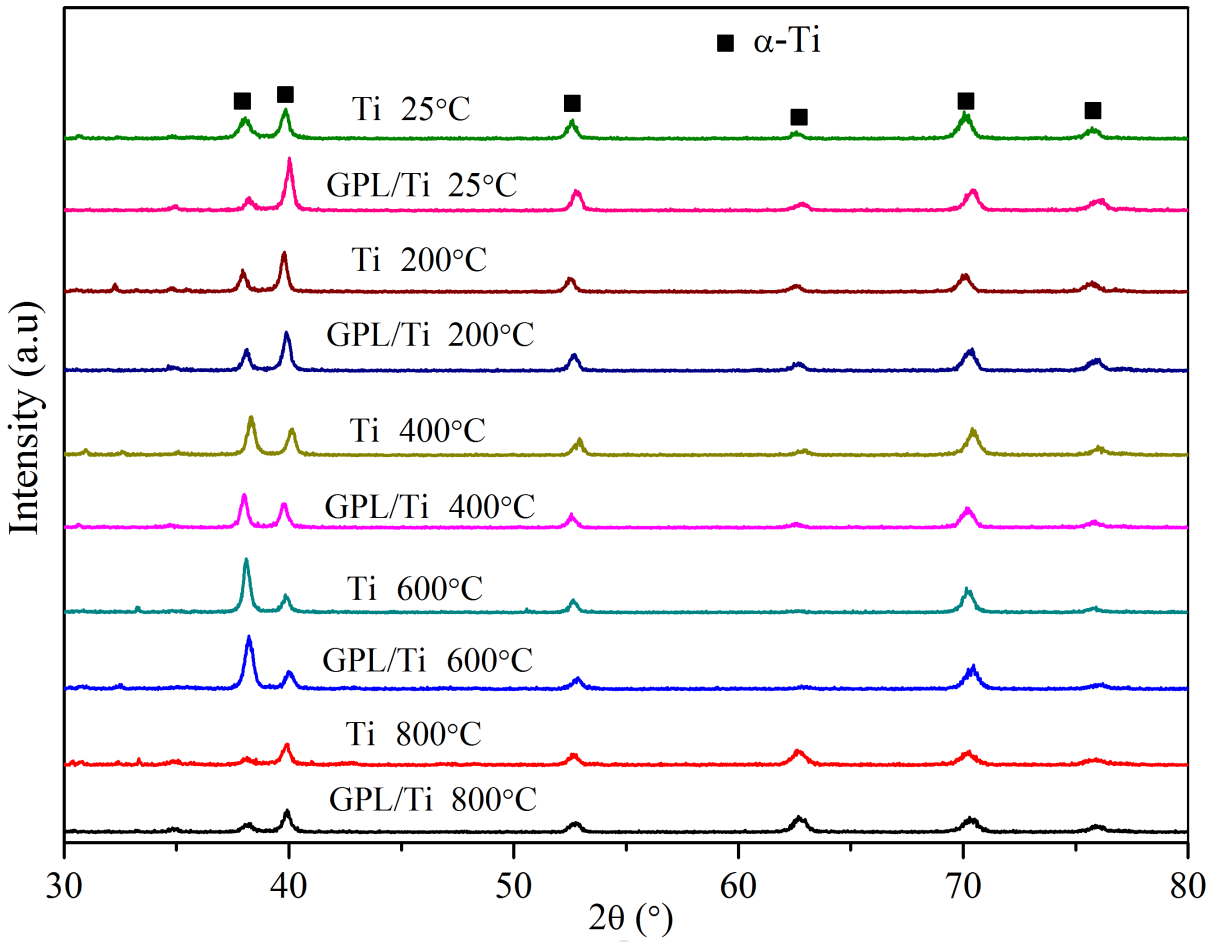

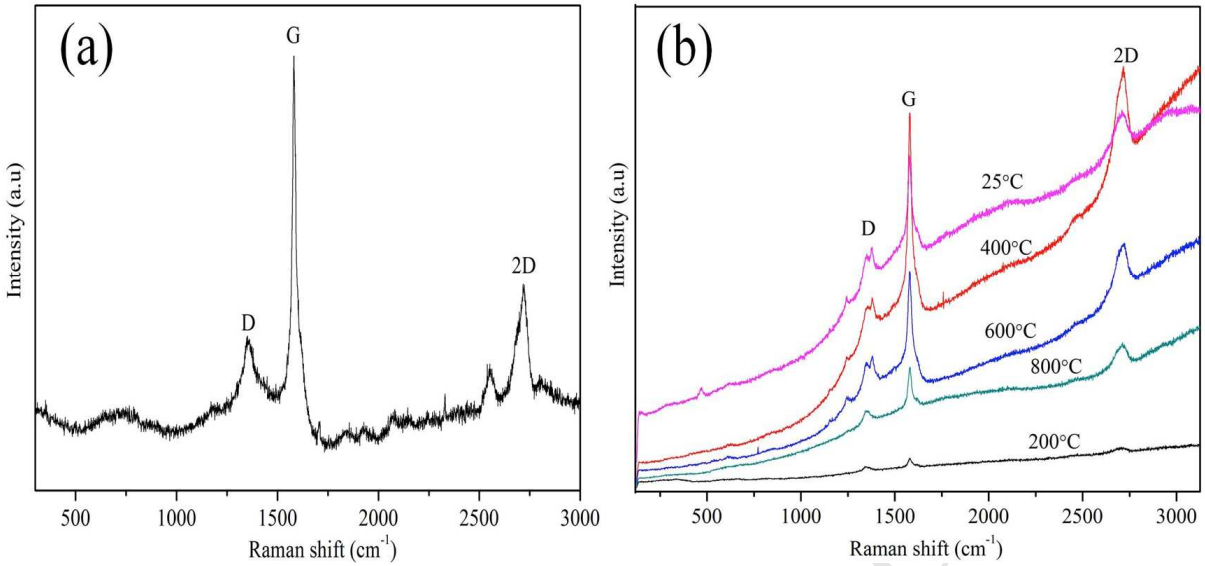

Highlights

Graphene/Titanium (GPL/Ti) composites were fabricated using sparking plasma sintering

GPL/Ti composites exhibit excellent compressive performance at various temperatures

GPL, TiC and the refined microstructure contribute to the attractive properties